Int J Thermophys (2011) 32:665–673
DOI 10.1007/s10765-011-0919-9

Effect of Solution Treatment on Thermal Conductivity of Porous NiTi Shape Memory Alloy

Mehmet Kaya · Abdulcelil Buğutekin · Nuri Orhan

Received: 13 May 2010 / Accepted: 11 January 2011 / Published online: 26 January 2011

Abstract In this study, a new solution treatment "solution treatment under loading" was applied to a porous Ni–50 at.%Ti shape memory alloy (SMA), which was fabricated by self-propagating high-temperature synthesis (SHS), to explore the microstructural improvement regarding single-phase NiTi. The effects of solution treatment under loading and without loading on the phase constituent and thermal conductivity were investigated and discussed. The phase constituent and thermal conductivity of the specimens considerably changed with solution treatment under loading, but they were not affected significantly with solution treatment without loading. Intermetallic phases such as B19′(NiTi), Ti_2Ni, and Ni_4Ti_3 disappeared, the density of the B2(NiTi) phase increased with solution treatment under loading, and thus the thermal conductivity was increased. It was also seen that the thermal conductivity of porous NiTi was less than that of solid NiTi.

Keywords Fourier Law · Porous NiTi · Solution treatment under loading · Thermal conductivity

M. Kaya (✉) · A. Buğutekin
Vocational School, Adiyaman University, 02040 Adiyaman, Turkey
e-mail: mkaya@adiyaman.edu.tr

A. Buğutekin
e-mail: abugutekin@adiyaman.edu.tr

N. Orhan
Metal Department, Technical Education Faculty, Firat University, 23119 Elazig, Turkey
e-mail: norhan@firat.edu.tr

1 Introduction

The NiTi intermetallics attract extensive interest because of their excellent mechanical properties, unique shape memory effect and superelasticity, good corrosion resistance, superior damping capability, and high biocompatibility [1]. Recently, the production of NiTi shape memory alloys (SMAs) as porous materials has received considerable interest due to their porous structures and extraordinary mechanical characteristics similar to those of some natural biomaterials for hard tissue implants [2,3].

Porous NiTi SMAs have been fabricated with powder metallurgy (PM) processes, such as self-propagating high-temperature synthesis (SHS), [4,5] metal injection molding [6], hot isostatic pressing [6,7], and spark plasma sintering [8], so far. However, none of the above PM processes has produced fully dense high-purity single-phase NiTi components [9]. The fully austenitic NiTi, B2(NiTi), material has suitable properties for surgical implantation and superelasticity [10]. A porous single-phase B2(NiTi) SMA with high chemical homogeneity could be obtained by the load applied during solution treatment at 1050 °C [11].

The thermal conductivity and mechanical properties of NiTi depend on its phase state at a certain temperature [10]. The thermal conductivity is required to determine the feasibility and the basic design parameters of structural materials [12]. Heat transfer refers to the energy transfer between two bodies due to a temperature difference. The energy is transferred from the high-temperature region to the low-temperature region due to random molecular motion–diffusion. Higher temperatures are associated with higher molecular energies, and when they collide with less energetic molecules, the transfer of energy occurs [13].

The heat transfer rate by conduction can be expressed as

$$q = -kA\left(\frac{\mathrm{d}T}{\mathrm{d}x}\right) \tag{1}$$

where q is the heat transfer rate (W), $\frac{\mathrm{d}T}{\mathrm{d}x}$ is the temperature gradient in the direction of the flow ($\mathrm{K}\cdot\mathrm{m}^{-1}$), k is the thermal conductivity of the material ($\mathrm{W}\cdot\mathrm{m}^{-1}\cdot\mathrm{K}^{-1}$), and A is the cross-sectional area of the heat path.

Equation 1 is known as Fourier's law of heat conduction. Therefore, the heat transfer rate by conduction through the specimen can be expressed as

$$q = \left(\frac{kA}{L}\right)\Delta T_{12} \tag{2}$$

where A is the cross-sectional area of the object, L is the wall thickness, ΔT_{12} is the temperature difference between two surfaces ($\Delta T_{12} = T_1 - T_2$), and k is the thermal conductivity of the object material ($\mathrm{W}\cdot\mathrm{m}^{-1}\cdot\mathrm{K}^{-1}$).

In our previous study [11], a porous Ni–49.5 at.%Ti SMA was fabricated by SHS and it was determined that the second phases such as Ti_2Ni and Ni_4Ti_3 could be eliminated completely and the single-phase B2(NiTi) occurred by solution treatment under

loading. In this study, the effects of solution treatment under loading and without loading on the phase constituent and thermal conductivity were investigated and discussed.

2 Experimental Procedures

A porous Ni–50 at.%Ti alloy with a porosity of 55.7 % was fabricated by SHS, for which the fabrication was explained in detail in our previous study [14]. To investigate the effects of solution treatment under loading and without loading on the phase constituent and thermal conductivity, fabricated specimens were separately solution treated under a load of 50 kg (6.41 MPa) and without loading at 1050 °C for 1 h in a furnace under the protection of high-purity argon gas. After that, the specimens were quenched into water at room temperature. In this study, the porosity of the solution-treated specimen under loading was determined as 40.9 %. The porosity is determined by the formula, $f = 1 - m/(dV)$, where V and m are the volume and mass of the porous specimen, respectively, and d is the theoretical density of it [14]. The porosity decreased with the solution treatment under loading, but it was insignificantly affected with solution treatment without loading.

The phase constituents of fabricated specimens and solution-treated specimens were determined by X-ray diffraction (XRD, Rigako Rad-B D-Max 2000 XRD) analysis using CuKα radiation with 1.54046 Å. Thermal-conductivity measurements of the specimens were tested with an H940 heat conduction unit (see setup, Fig. 1). Different views of the H940 heat conduction unit are seen in our previous study [15]. First, a 316 stainless-steel specimen whose thermal conductivity is known was tested to understand the accuracy of the measurements, and then the specimens were tested. The thermal conductivity of the 316 stainless-steel specimen was 14.8 $W \cdot m^{-1} \cdot K^{-1}$ near room temperature and increased to 17.5 $W \cdot m^{-1} \cdot K^{-1}$ with increasing temperature. These values are consistent with literature values [16]. The specimens were disks of 10 mm in diameter and 5 mm in thickness. First, the specimens were isolated with polyurethane spray about 1 mm thick to prevent convection losses (also, protective boxes with heat-resistance were used to prevent heat losses), and then both sides of the specimens were polished to create good contact with the surfaces of brass plates. After the specimens were placed between two brass plates, one of them was heated with a power supply and the other cooled with running water. Thus, heat was transferred from the heated brass to the cooled brass. The experiments were carried out in an air atmosphere. The temperature changes were measured as a function of time by thermocouples. The thermocouples were placed apart at a distance of 10 mm on the brass plates. Temperature values with a sensitivity of ± 1 °C on a digital screen were recorded, and the power was controlled between (0 and 100) W. Thermal conductivities of the specimens were determined with Fourier's law of heat conduction. ΔT_{12} in Eq. 2 is selected as $\Delta T_{45} = T_4 - T_5$ in Fig. 1.

3 Results and Discussion

The XRD patterns of the fabricated specimen, the specimen solution treated without loading, and the specimen solution treated under loading are shown in Fig. 2a, b, c,

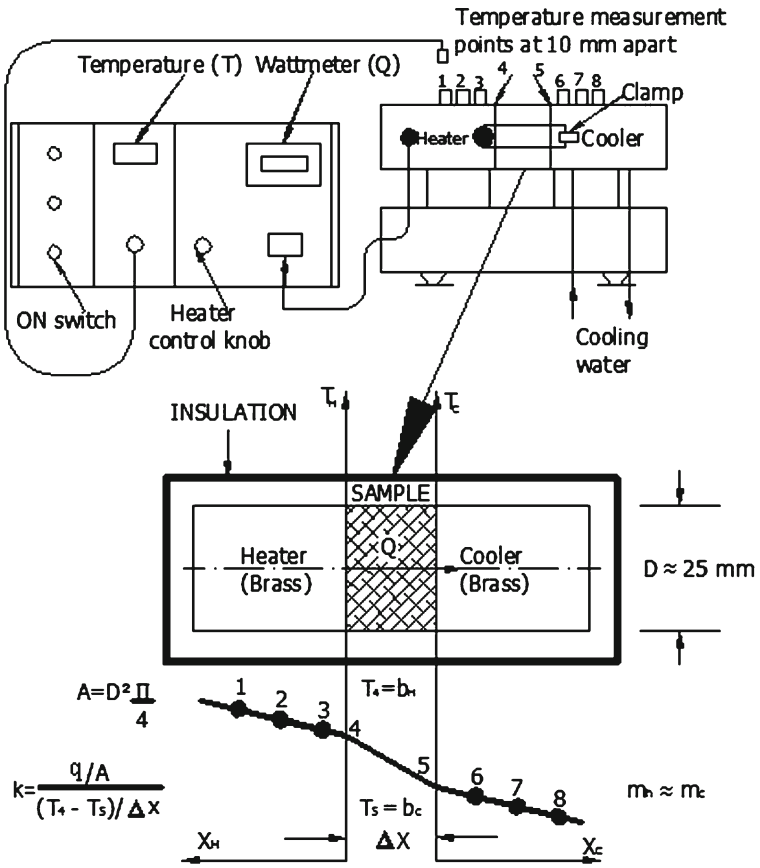

Fig. 1 Setup of the thermal-conductivity measurement, also, different views of H940 heat conduction unit can be seen in our previous study [15]

respectively. The desired products, such as B2(NiTi) and B19′(NiTi), are the predominant phases in the porous NiTi alloy fabricated by SHS. In addition, several second phases, such as Ti_2Ni and Ti_3Ni_4, are also formed (Fig. 2a). The same phases were explored by Chu et al. [17]. In addition, they reported that the amount of the metastable Ni_4Ti_3 phase decreased sharply after solution heat treatment at 1050 °C for 4 h, and the Ti_2Ni phase could not be removed by solution treatment [17]. Ti_2Ni, Ni_3Ti, and Ni_4Ti_3 phases existing in a SHS-synthesized porous NiTi SMA may increase the brittleness of the products. Moreover, they can lead to galvanic corrosion and deteriorate the biocompatibility of porous NiTi SMAs in physiological environments [17,18]. Therefore, these second phases are undesired.

It can be seen that constituents of Ti_3Ni_4 and B19′(NiTi) phases decreased and the B2(NiTi) phase increased, but the amount of the Ti_2Ni phase was not effected considerably (Fig. 2b); also, it can be seen in Fig. 2c that single-phase B2(NiTi) occurred. The single-phase B2(NiTi) occurred when solution treatment and load were applied together. In other words, Ni_4Ti_3, Ti_2Ni, and B19′(NiTi) phases disappeared and the

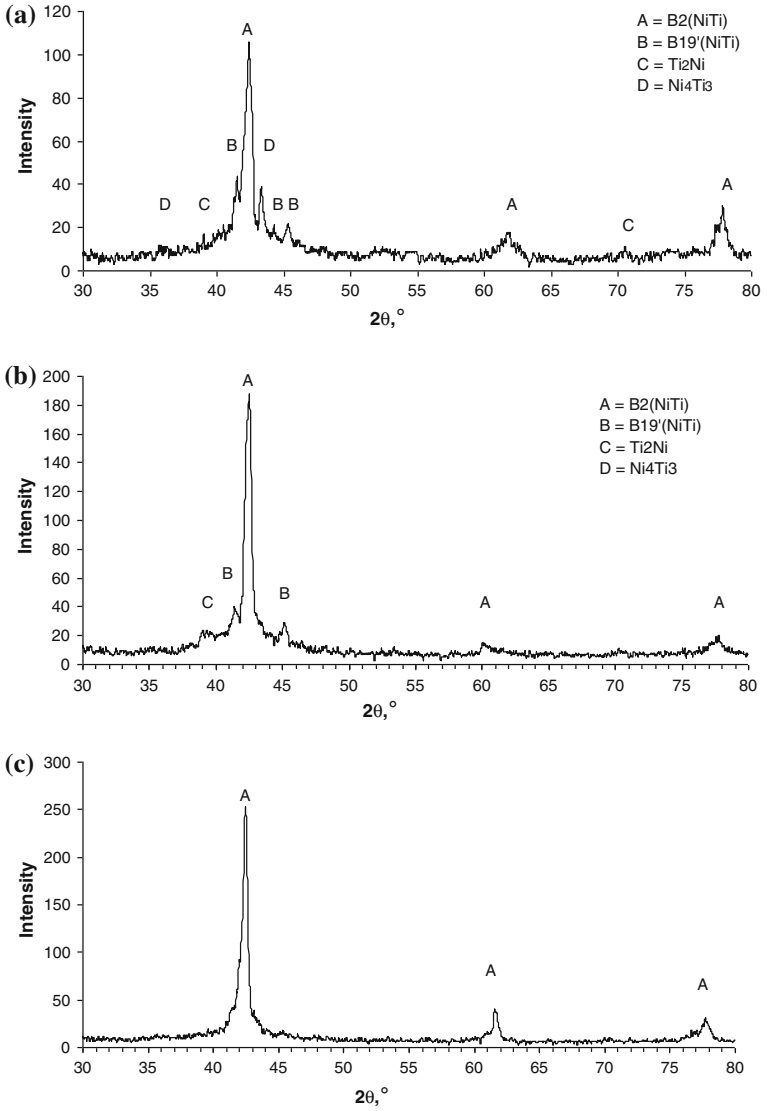

Fig. 2 XRD patterns of porous NiTi SMAs: (a) the fabricated specimen, (b) the specimen solution treated at 1050 °C for 1 h, without load, and (c) the specimen solution treated with an applied load of 6.41 MPa at 1050 °C for 1 h

microstructure transformed into the B2(NiTi) phase with solution treatment under loading. Similar conclusions were determined for porous Ni–49.5 at.%Ti fabricated by SHS after solution treatment under loading [11].

The typical variations of temperature with time within the specimens for T_4 and T_5 locations are seen in Table 1 and Fig. 3. The results indicate that the temperature variations between T_4 and T_5 locations increased directly with increasing time, and

Table 1 Typical variations of temperature and thermal conductivity with time within the specimens: for (a) the specimen fabricated by SHS, (b) the solution-treated specimen without loading, and (c) the solution-treated specimen under loading

Time (min)	Heat rate (W)	T_4 (°C)	T_5 (°C)	k (W · m^{-1} · K^{-1})
(a)				
30	10	243.2	22.3	337.38
60	10	59.5	19.4	15.98
90	10	87.6	17.6	9.15
120	9.7	103.5	15.4	7.05
150	9.7	104.3	15.2	6.97
180	9.6	105.4	15.3	6.83
220	9.7	105.7	15.2	6.87
240	9.7	105.8	15.3	6.87
(b)				
30	10	24.2	22.3	337.38
60	10	57.6	19.8	16.95
90	9.6	81.2	18.7	9.84
120	9.6	96.5	17.8	7.81
150	9.7	99.7	17.1	7.52
180	9.6	101.2	16.8	7.29
220	9.7	10.1	16.7	7.36
240	9.8	101.3	16.8	7.43
(c)				
30	10	24.4	22.3	305.25
60	10.1	56.5	21.1	18.28
90	10.1	75.6	20.4	11.72
120	10.2	78.6	19.7	11.10
150	9.5	78.6	19.8	11.01
180	10.2	78.7	19.6	11.06
220	10.1	78.5	19.7	11.01
240	10.1	78.4	19.8	11.04

after this, the temperature variations were uniform after about 120 min. In general, steady-state temperatures were obtained after about 120 min. This time period is a function of the properties of the used specimen, the heating rate, and the geometry of the apparatus. The thermal conductivities of the specimens were defined with Eq. 2, using the temperatures and heating rates after this time period. The temperature variations between T_4 and T_5 locations of the specimen fabricated by SHS were highest, but the temperature variations of the same locations of the solution-treated specimens under loading were lowest. These results indicate that the thermal conductivity of the fabricated specimen is lowest and the thermal conductivity of the solution treated specimen under loading is highest. It was determined that the thermal conductivities were (6.9, 7.4, and 11.4) W · m^{-1} · K^{-1} for the fabricated specimen,

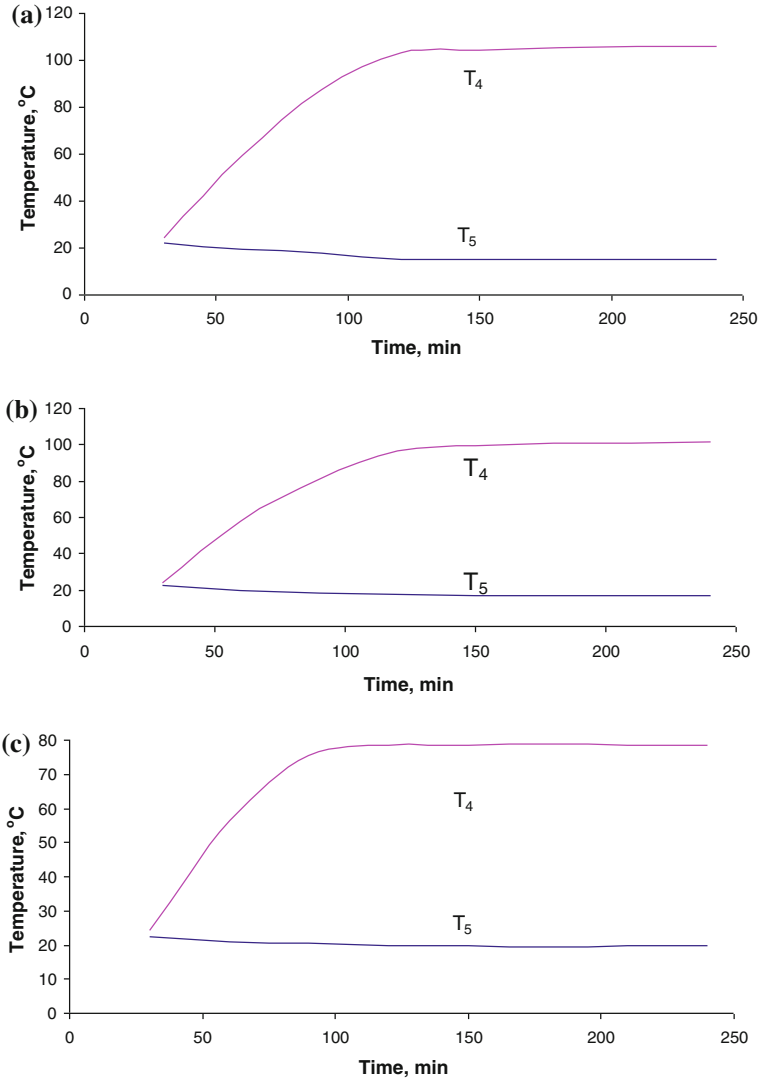

Fig. 3 Typical variations of temperatures with time within the specimens for T_4 and T_5 locations: (a) specimen fabricated by SHS, (b) solution-treated specimen without loading, and (c) solution-treated specimen under loading

the solution-treated specimen without loading, and the solution-treated specimen under loading, respectively.

In this study, the porosity of the fabricated specimen and the solution-treated specimen was the same (55.7 %), but the B2(NiTi) phase increased and the B19′(NiTi) and Ni_4Ti_3 phases decreased with a solution-treated specimen. It can be understood that the B2(NiTi) phase resulted in an increased thermal conductivity while B19′(NiTi) and Ni_4Ti_3 phases resulted in a decreased thermal conductivity because

the thermal conductivity of the fabricated specimen was lower than that of the solution-treated specimen. The fabricated specimen contains the phases such as B2(NiTi), B19′(NiTi), Ti_2Ni, and Ni_4Ti_3 while the solution-treated specimen under loading contains only single-phase B2(NiTi). The thermal conductivity of the solution-treated specimen under loading is highest due to this specimen's existing single phase B2(NiTi), and its porosity is lowest. It can be understood that the thermal conductivity of single-phase B2(NiTi), austenite, is higher than that of existing multiphases of the NiTi alloy. Similar results are found in the literature [19]. The thermal conductivity of the solid NiTi wire's existing B19′(NiTi) phase, martensite, is $14\,W \cdot m^{-1} \cdot K^{-1}$ while the thermal conductivity of the solid NiTi wire's existing B2(NiTi) phase, austenite, is $24\,W \cdot m^{-1} \cdot K^{-1}$ [19]. In this study, it is seen that the thermal conductivities of the porous specimens are lower than that of the solid specimen. Similar results were determined by Zanotti et al. [20], for which the thermal conductivity decreased with increasing porosity. They determined that the thermal conductivity for porous NiTi with a porosity of 68 %, 48 %, and 30 % were about (4, 3, and 2) $W \cdot m^{-1} \cdot K^{-1}$, respectively. These values are lower than those in this study due to their specimens containing multiphases. Also, the experimental conditions of the measurements were different from those in this study.

4 Conclusions

1. Solution treatment increased the constituent of the B2(NiTi) phase and decreased the constituents of Ni_4Ti_3 and B19′(NiTi) phases in the microstructure of NiTi SMA, but the amount of the Ti_2Ni phase was not significantly affected with solution treatment without loading.
2. The solution-treated specimen under loading had a single-phase B2(NiTi) while the specimen fabricated by SHS had intermetallics such as Ni_4Ti_3, Ti_2Ni, B19′(NiTi), and B2(NiTi). In the case of loading during the solution treatment, undesired intermetallics such as Ni_4Ti_3, Ti_2Ni, and B19′(NiTi) phases disappeared and the microstructure transformed to the B2(NiTi) phase. A porous single-phase B2(NiTi) with high chemical homogeneity was obtained by the load applied during solution treatment.
3. It was found that the thermal conductivity of a solution-treated specimen was higher than that of the specimen fabricated by SHS. In addition, it was seen that the thermal conductivity of B2(NiTi) was the highest, and the thermal conductivity of porous NiTi was lower than that of solid NiTi.

Acknowledgment The authors thank Marmara University, Technical Education Faculty, Department of Energy for support on thermal conductivity measurements of the specimens, which were tested with an H940 heat conduction unit.

References

1. C.L. Yeh, W.Y. Sung, J. Alloys Compd. **376**, 79 (2004)
2. C.L. Chu, C.Y. Chung, P.H. Lin, S.D. Wang, J. Mater. Process. Technol. **169**, 103 (2005)
3. H.C. Man, S. Zhang, F.T. Cheng, X. Guo, Mater. Sci. Eng. A **404**, 173 (2005)

4. H.C. Jiang, L.J. Rong, Mater. Sci. Eng. A **438**, 883 (2006)
5. M. Whitney, S.F. Corbin, R.B. Gorbet, Acta Mater. **56**, 559 (2008)
6. L. Krone, E. Schüller, M. Bram, O. Hamed, H.P. Buchkremer, D. Stöver, Mater. Sci. Eng. A **378**, 185 (2004)
7. B. Yuan, C.Y. Chung, M. Zhu, Mater. Sci. Eng. A **382**, 181 (2004)
8. C. Shearwood, Y.Q. Fu, L. Yu, K.A. Khor, Scripta Mater. **52**, 455 (2005)
9. B. Bertheville, J.E. Bidaux, J. Alloys Compd. **387**, 211 (2005)
10. J. Ryhanen, *Biocompatibility Evaluation of Nickel-Titanium Shape Memory Metal Alloy* (Oulun Yliopisto, Oulu, 1999). http://herkules.oulu.fi/issn03553221
11. M. Kaya, N. Orhan, B. Kurt, T.I. Khan, J. Alloys Compd. **475**, 378 (2009)
12. Y. Terada, K. Ohkubo, S. Miura, J.M. Sanchez, T. Mohri, J. Alloys Compd. **354**, 202 (2003)
13. A. Buğutekin, B. Köse, A.K. Binark, M.O. Isıkan, Application Insulation Technologies Congress (İstanbul, Turkey, 2005), pp. 875–879
14. M. Kaya, N. Orhan, G. Tosun, Curr. Opin. Solid State Mater. Sci. **14**, 21 (2010)
15. M. Kaya, A. Bugutekin, N. Orhan, Optoelectron. Adv. Mater. Rapid Commun. **4**, 1250 (2010)
16. L.J. Ott, R.A. Hedrick, *ORTCAL- A Code for THTF Heater Rod, Thermocouple Calibration* (Oak Ridge National Laboratory, TN, 1979), p. 217
17. C.L. Chu, J.C.Y. Chung, P.K. Chu, Trans. Nonferrous Metal Soc. China **16**, 49 (2006)
18. P. Sevilla, C. Aparicio, J.A. Planell, F.J. Gil, J. Alloys Compd. **439**, 67 (2007)
19. M.G. Faulkner, J.J. Amalraj, A. Bhattacharyya, Smart Mater. Struct. **9**, 632 (2000)
20. C. Zanotti, P. Giuliani, P. Bassani, Z. Zhang, A. Chrysanthou, Intermetallics **18**, 14 (2010)